

Spectral signature of mass outflow in Two Component Advective Flow Paradigm

SANTANU MONDAL^{*1} AND SANDIP K. CHAKRABARTI²¹*Indian Institute of Astrophysics, II Block, Koramangala,
Bangalore 560034, India*²*Indian Centre for Space Physics, 43 Chalantika,
Garia Stn. Road, Kolkata 700084, India*

ABSTRACT

Outflows are common in many astrophysical systems. In the Two Component Advective Flow (TCAF) paradigm which is essentially a generalized Bondi flow including rotation, viscosity and cooling effects, the outflow is originated from the hot, puffed up, post-shock region at the inner edge of the accretion disk. We consider this region to be the base of the jet carrying away matter with high velocity. In this paper, we study the spectral properties of black holes using TCAF which includes also a jet (JeTCAF) in the vertical direction of the disk plane. Soft photons from the Keplerian disk are up-scattered by the post-shock region as well as by the base of the jet and are emitted as hard radiation. We also include the bulk motion Comptonization effect by the diverging flow of jet. Our self-consistent accretion-ejection solution shows how the spectrum from the base of the jet varies with accretion rates, geometry of the flow and the collimation factor of the jet. We apply the solution to a jetted candidate GS 1354-64 to estimate its mass outflow rate and the geometric configuration of the flow during 2015 outburst using *NuSTAR* observation. The estimated mass outflow to mass inflow rate is $0.12^{+0.02}_{-0.03}$. From the model fitted accretion rates, shock compression ratio and the energy spectral index, we identify the presence of hard and intermediate spectral states of the outburst. Our model fitted jet collimation factor (f_{col}) is found to be $0.47^{+0.09}_{-0.09}$.

Keywords: black hole physics — accretion disk — shock waves — hydrodynamics — ISM:jets and outflows — star:individual GS 1354-64

1. INTRODUCTION

Observations show that jets are common in active galactic nuclei (AGN), stellar mass black holes and neutron stars (e.g., Hjellming & Rupen 1995; Mirabel & Rodríguez 1998; Miller-Jones et al. 2012; Blandford et al. 2019, and references therein). A proper understanding of the origin and acceleration of jets in compact objects is, however, lacking till date. Several models in the literature attempt to explain the origin, powering, and collimation of the jet. D'Silva & Chakrabarti (1994) suggested that only the dominant toroidal field in the disk would be enough to accelerate and collimate the jets. This has been recently verified using numerical simulation by Garain et al. (2020). Fender et al. (2010) from their observational

studies did not find any evidence of jet powered by the spin energy of the black holes and the authors speculated that this conclusion remained valid even for active galaxies and quasar. On the contrary, Narayan & McClintock (2012) found a correlation between jet power and black hole spin energy. Thus, the role of spin parameter in powering jet is still unclear and more studies must be done to reach a firm conclusion. The hydrodynamic jets can also be collimated due to the strength of the jet-cocoon interaction and the collimation shock at the base of the jet (Bromberg et al. 2011).

Therefore, accretion-ejection around black hole systems has three components: the accretion disk, its static or dynamic corona, and the outflowing jet. It is well established that the standard disk (Shakura & Sunyaev 1973) emits soft photons, up-scattered by the hot Compton cloud at the inner region of the disk and emit as hard radiation. The emergent radiation may get down-scattered by the diverging outflows for both sub-

and super-Eddington accretion (Kawashima et al. 2012; Titarchuk & Shrader 2005, hereafter TS05). This effect changes the intrinsic continuum spectra of accretion disks with an additional bump (Sunyaev & Titarchuk 1980) in the powerlaw spectrum. The problem of photon propagation through a moving medium has been studied extensively in several works (Blandford & Payne 1981; Nobili et al. 1993; Titarchuk et al. 2003). There are numerous studies on this context in the literature, both in theory and radiation hydrodynamic simulation (Eggum et al. 1988; King et al. 2001; Okuda 2002; Ebisawa et al. 2003; Ohsuga et al. 2005). In addition to down-scattering of hard radiation, jet can also behave like an up-scattering Comptonizing medium of the soft photons from the disk. The presence of soft-excess is a commonly observed spectral component for both X-ray binaries and AGNs. This can be originated if there is some warm Compton up-scattering medium is present in the system. The excess component can also be associated as an intrinsic component with the disk, powered by the mass accretion rate (Done et al. 2012), appeared as a reflection component (Done et al. 2007, for a review). This distortion of the power-law continuum above ~ 10 keV energy could also be due to down-scattering of hard radiation by the outflowing plasma rather than from a static reflecting medium (TS05). In addition to these spectral features, a converging flow falling onto the black hole near the event horizon can show bulk motion effect (Chakrabarti & Titarchuk 1995; Titarchuk & Zannias 1998, hereafter CT95). Under such a complex radiation components coming from the accretion-ejection system, it is important to ask, independent of how a jet is launched from the disk, what would be the overall X-ray spectrum in the presence of a jet, and what is the contribution from the base of the jet itself, specially the subsonic region which is hot. Most importantly, whether there is any evidence of such a contribution.

Chakrabarti (1999, hereafter C99) postulated that the jets in the black hole systems are formed out of the post-shock region, which is also called the CENtrifugal pressure dominated BOundary Layer or CENBOL. This is the subsonic, hot region between the shock and the inner sonic point (Chakrabarti 1989) located just inside the marginally stable orbit. C99 also proposed that the entire outflow is produced by the CENBOL and the mass outflow rate directly depends on the compression ratio $R = \frac{\rho_+}{\rho_-}$ of the shock itself, where ρ_- and ρ_+ are the densities of the flow in the pre-shock and post-shock regions. It was shown that the ratio of the mass outflow rate to inflow rate is indeed a function of R varies in a non-linear way apart from a geometric factor coming from the solid

angles of the outflow and the inflow. For a very strong shock, which forms farther out as in a hard state, the thermal driving force is low and the jet is not powerful. Similarly, in a soft state, when the shock is the weakest, the size of the base of the jet is negligibly small, thermal driving force is also low and hence the ratio is also low. Only in between the two states, the ratio is significant. Several hydrodynamic simulations showed that a few percent of accreting matter is indeed present in the jet (Molteni et al. 1994; Chattopadhyay et al. 2004; Garain et al. 2012). Singh & Chakrabarti (2011) studied jet properties of the flow when the energy dissipation is present at the shock and found lower efficiency of the jet formation when viscosity is high.

In Chakrabarti (1997) two component flow scenario, it is established that the emission from the CENBOL decreases as the accretion rate of the Keplerian disk is increased, both because its size and temperature are reduced. This reduction of thermal pressure of CENBOL reduces the mass outflow rate. Thus, accretion rates, spectral states, and jet are interlinked. Observations evidenced prominent jets in hard and hard-intermediate spectral states (HS and HIMS, Fender et al. (2004)). Transonic solution including real cooling (Mondal & Chakrabarti 2013) and outflows (Mondal et al. 2014a) showed that spectral states are related to mass outflow rate and a significant change in energy spectral index are observed in HS and HIMS. These solutions are self-consistent in the sense that cooling and mass loss are incorporated in the flow equations before obtaining the spectra. Recent work by Nagarkoti & Chakrabarti (2016) using a viscous solution confirms that a significant amount of mass loss is centrifugally driven as suggested by Blandford & Payne (1982) though the disk may be sub-Keplerian in nature.

The interdependency between the accretion rate, CENBOL size and QPOs is also well known in the literature. During an outburst, when a source moves from HIMS to SIMS, the QPO type switches from type-C to type-B (e.g., Mondal et al. 2014b; Debnath et al. 2015; Chatterjee et al. 2016, and references therein). However, jet properties also changed drastically, which is observed in large amplitude radio flares (Fender et al. 2004, 2009). Radhika & Nandi (2014) reported the accretion-ejection mechanism for the object XTE J1859+226 and pointed out that the quasi-periodic-oscillations (QPOs) disappear during the high ejection of jets. All these are expected from the TCAF paradigm, since QPOs are known to be formed due to the resonance of various time scales inside CENBOL which also produces jets. Interestingly, the highest outflow to inflow rate from the theoretical solution

of C99 happens for intermediate compression ratio of the shock, i.e., in hard and soft-intermediate states. Retaining CENBOL is possible only in a low viscosity state (Mondal et al. 2017).

The original TCAF solution of CT95 and C97 does not include the contribution from outflows and therefore, presence of significant outflows require a modification of the model. This is the primary goal of this paper. Here, we concentrate on the effects on the emergent spectra when the base of the outflow also participates in Comptonization of injected photons along with the CENBOL. We study the jet spectrum when the accretion rates, the geometry of the flow and jet parameters vary. We also see the variation of the spectra from the jet with the variation of CENBOL size and shock compression ratio. The study of optical and radio observations (Brocksopp et al. 2001; Pahari et al. 2017) inferred the presence of jet in GS 1354-64 system, however, there is very little study on this object as far as the effects of jets are concerned. We apply the solution to study this object, in order to throw some light on accretion-ejection behavior during its 2015 outburst. In fact, from the fits of the modified TCAF model, we extract the jet parameters, such as the mass outflow rate, as well. In future, we aim to apply the solution to other well known candidates which exhibit prominent jets.

The paper is organized as follows: in the next Section, we present the configuration of the jet and the equations we used to calculate jet temperature and internal number density, etc. In §3, we present the results of the effects of mass loss on normal in TCAF output, mainly the spectral variation with location of the shock, shock compression ratio and accretion rates. In §4, we calculate the mass outflow rate of the BHC GS 1354-64 during its 2015 outburst using *NuSTAR* observation. Finally, in §5, we briefly present our concluding remarks.

2. EQUATIONS AND JET CONFIGURATION

To extract the jet properties from a spectral fit, we consider a conical jet in the vertical direction of the flow, which is originated from the post-shock region. The base of the jet is a part of the Compton cloud along with the CENBOL. In Figure 1, we present a cartoon diagram of the two-component flow with a jet where a Keplerian disk resides at the equatorial plane, and it is surrounded by the low angular momentum flow (dynamic halo). At the center, a black hole of mass M_{BH} is located. We show also the solid angles Θ_o and Θ_{in} subtended by the two outflow components and the axisymmetric torus created by the CENBOL respectively.

The spectrum emitted from the system contains (a) modified blackbody component, which is coming from

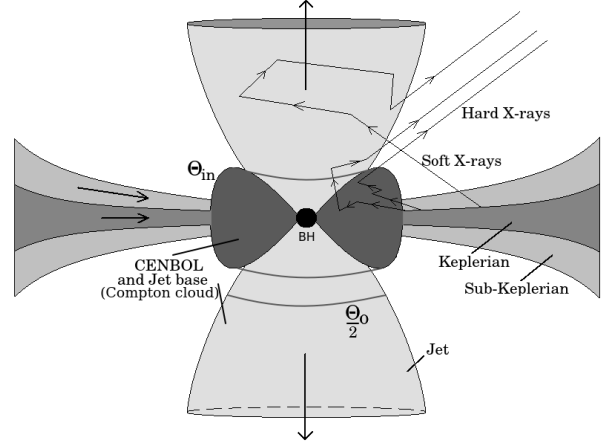


Figure 1. A cartoon diagram of the geometry of an accretion flow with a jet in the vertical direction. Here, Θ_o and Θ_{in} are solid angles subtended by the outflow and the CENBOL respectively. The base of the jet is treated as a Comptonizing medium, which also contributes in computing model spectra. Zigzag trajectories are the typical paths followed by soft photons from the Keplerian disk. These photons are Comptonized by the CENBOL and the jet base (marked) and are radiated as hard X-rays.

the Keplerian disk, (b) the soft photons from the disk are up-scattered by the hot electrons at the inner region of the disk and come out as hard radiation, (c) disk soft photons also get up-scattered by the jet base, which modifies the spectrum on the shoulder of the blackbody bump, and (d) hard radiation from the CENBOL are down-scattered by the outflowing jet due to Doppler effect. The components (a) and (b) are already computed in the original Chakrabarti & Titarchuk (1995) paper. For the component (c) we use the same radiative transfer calculation incorporating the temperature and optical depth of the jet. Once we have the physical quantities of the jet medium and the spectral component (b), we use it to pass through the jet medium following TS05. Below, we discuss the equations used to estimate different physical quantities of the jet medium.

The radiation from the CENBOL may constantly heat up the jet and the jet may not get enough time to cool at least up to the sonic point. Thus, the ratio of the mass outflow rate to the mass inflow rate is derived for an isothermal base of the jet (C99), which is given by,

$$\dot{M}_{\text{out}} = f_{\text{col}} f_0^{3/2} \frac{R}{4} \exp \left[\frac{3}{2} - f_0 \right], \quad (1)$$

where, $f_0 = \frac{R^2}{R-1}$ and $f_{\text{col}} (= \Theta_o / \Theta_{\text{in}})$ is the collimation factor. Here, Θ_o and Θ_{in} are the solid angles subtended by the two outflow components and the inflow. We should mention that f_0 factor diverges when $R \sim 1$. However, that does not create any complications in produc-

ing the spectrum, since when $R \sim 1$, the flow is not a TCAF and produces the blackbody spectrum only. It is clear that the mass outflow rate is a function of only R and f_{col} . Here, f_{col} is a parameter and its value is varied in the range (see Table 1) to fit the observed data. One of the values of f_{col} is 0.1, which corresponds to $\Theta_o \sim 10^\circ$. Molteni et al. (1994) discussed that Θ_o , should depend on the strength of the centrifugal barrier. If the barrier is stronger, Θ_o and consequently the mass loss rate is higher. The total accretion rate of the in-flowing matter at the CENBOL after mixing of the Keplerian and sub-Keplerian components is given by,

$$\dot{M}_{\text{in}} = \dot{M}_{\text{d}} + R\dot{M}_{\text{h}}, \quad (2)$$

here, \dot{M}_{d} and \dot{M}_{h} are the disk and halo rates respectively of the flow in gmsec^{-1} unit. Since in TCAF, the boundary layer, i.e., CENBOL, is emitting the jet, the initial launching velocity of the ejecta comes from the temperature of the post-shock region, i.e., $v_j \sim \sqrt{T_{\text{shk}}} \sim 0.1c$. However, it changes depending on the CENBOL location. The density at the base of the jet is calculated using,

$$\rho_{j0} = \frac{\dot{M}_j}{\pi X_s^2 v_j}, \quad (3)$$

where, $\dot{M}_j (= R_{\text{in}} \dot{M}_{\text{in}})$ is the rate of the mass outflow. As the height increases, density of the outflowing matter falls as,

$$\rho_j = \rho_{j0} \left(\frac{r_j}{r_{j0}} \right)^{-2}, \quad (4)$$

where, r_j and $r_{j0} (= h_{\text{shk}})$ are the (running) height of the jet and the fixed height of the base of the jet respectively. The latter is basically the height of the shock (h_{shk}). We assume that the jet matter moves away subsonically till the sonic surface, the radius of which is given by (C99),

$$r_c = \frac{f_0 X_s}{2}. \quad (5)$$

We assume that the temperature of the jet (T_j) varies as $\sim 1/r_j$. In this work, we also consider the effects of down-scattering of the Comptonized photons by the bulk motion of the outflowing jet as discussed in TS05. There are a number of sources which show evidence of strong reflection above ~ 10 keV. This distortion of the power-law continuum above this energy can also be originated from the down-scattering of the hard radiation by the outflowing plasma rather than from a static reflecting medium. This is discussed in CT95 and TS05. Here, we implement this to explain the excess radiation component present in the spectrum. We use the following equation from TS05 for the final down-scattered jet

Table 1. JeTCAF model parameters range

Pars.	Units	Default	Min.	Min.	Max.	Max.	Increment
M_{BH}	M_\odot	6.0	4.0	4.0	15.0	15.0	2.0
\dot{m}_{d}	\dot{M}_{Edd}	0.01	0.001	0.001	2.0	2.0	0.05
\dot{m}_{h}	\dot{M}_{Edd}	0.1	0.001	0.001	5.0	5.0	0.2
X_s	r_g	50.0	6.0	6.0	400.0	400.0	8.0
R	" "	2.1	1.1	1.1	7.0	7.1	0.2
f_{col}	" "	0.1	0.05	0.05	0.5	0.5	0.01

spectrum:

$$F_{\text{BMC}} \propto \Phi_{\text{Comp}} \left\{ 1 + N_{\text{av}} z \left[(1 - \alpha) - \frac{\epsilon}{3z_*} - \frac{z}{z_*} \right] \right\}, \quad (6)$$

where the second term in the bracket describes the pile-up and softening of the input Comptonization spectrum (Φ_{Comp}), resulting from the down scattering effect by the jet electrons. Here, $N_{\text{av}} (= 3\tau_0^2/8)$ is the number of average scattering, ϵ is the efficiency of the energy loss in the divergent flow ($\sim 2v_j/c\tau_0$), z is the dimensionless photons energy, z_* is the dimensionless temperature and τ_0 is the optical depth of the scattering medium, namely, the base of the jet. The Φ_{Comp} , we used here, is the spectrum emitted from the CENBOL due to up-scattering of disk soft photons and α is the energy spectral index estimated from the original TCAF code (CT95) to make the computation to be consistent. However, TS05 assumed this spectral component to be a cut-off power-law for a given α . The subscript BMC implies the bulk motion Comptonization.

The units of mass, length, speed, and accretion rates are M_\odot , $r_g = 2GM/c^2$, c , and \dot{M}_{Edd} respectively, where M_\odot , G , M_{BH} , c and \dot{M}_{Edd} are the mass of the Sun, gravitational constant, mass of the central object, speed of light and Eddington accretion rate. Throughout the paper we follow these units for model parameters and physical quantities.

3. RESULTS AND DISCUSSIONS

We show how the spectral properties change when the base of the jet is also a part of the Compton cloud. In Figure 2a, we show the spectral variation of the jet component from the total emitted spectrum for different accretion rates (\dot{m}_{d}), when other flow parameters (\dot{m}_{h} , M_{BH} , X_s and R) are kept constant. We increase the accretion rates, i.e., the number of soft photons and observe that the jet spectrum softens. Here, we used $f_{\text{col}}=0.1$ and other parameters are marked with figure. Increase in soft photon number also cools down the Compton cloud rapidly. Thus, the emitted jet does not have sufficient thermal energy to up-scatter the soft photons significantly. In Figure 2b, we present the spectra of different spectral states by varying the accretion rates only, keeping all other parameters fixed. Here the

spectra vary from HS to SS and the same variation is reflected in the jet contribution in the spectra as well. Spectral states may change due to different sizes of the cloud and compression ratio of the shock, since, these two physical parameters are also related to density and optical depth of the system.

Figure 3a shows the effects of the size of the Compton cloud ($X_s = 10, 20, 40$ and 60) on the jet component of the total emitted spectrum. We see that as the size of the cloud increases, the jet spectral component becomes softer. As the base of the jet is the CENBOL, the jet component varies with shock location. Larger CENBOL being farther from the black hole, its temperature is already less (roughly $\propto 1/X_s$). Also, it intercepts more soft photons from the Keplerian disk which reduces the overall CENBOL temperature (Chakrabarti 1997). Thus, the resulting temperature of the base of the jet becomes lower. Thus, the soft primary photons are not up-scattered many times. This causes the jet spectrum to be softer. In Figure 3b, we show the jet component variation for different values of R ($=2.0, 2.5, 3.5, 4.5$ and 6.0). We observe significant changes in the jet component, which becomes softer with increasing R . From C99 solution, we see that the mass outflow rate decreases when R is higher than ~ 4.0 . This affects the spectral shape, for instance, when $R = 6.0$, mass outflow rate is very low and consequently the spectrum is also softer. In Figure 3c, we see the spectral hardening when jet collimation factor (f_{col}) has changed from 0.05 to 0.3 .

Figure 4a shows the variation of the net spectrum with (solid) and without jet (dashed line) contribution as a function of the shock compression ratio (R). We note that due to the presence of the jet, the total spectrum becomes harder as compared to that without the jet. The variation of the total spectrum with R is significant. In Figure 4b, we show the total emitted spectra for different values of collimation factor. The dashed line shows the total spectrum when jet contribution is not included, and the solid colored lines are the total spectrum with the jet contribution. One can see that as the collimation factor increases, the spectrum becomes harder when the other parameters are fixed.

Figure 5a shows the total spectral variation of different states with (solid lines) and without (dotted lines) the jet contribution. Here the spectral state changes with accretion rates when other parameters of the model are kept fixed. As the accretion rate increases, more soft photons from the Keplerian disk are intercepted by the Compton cloud and the spectrum becomes softer. On the other hand, an increase in disk accretion rate cools down the CENBOL which reduces the thermal

pressure and thus reduces the mass outflow rate. Consequently, the system moves to the soft state through intermediate states. In Chakrabarti (1996), it was proposed that viscosity is mainly responsible for changing the relative rates, which is indirectly taken into account by two accretion rates in TCAF. In Mondal et al. (2017), it was shown that the observed viscosity parameter indeed rises in the rising phase and decreases in the declining phase, thereby completing the full cycle of the observed states. In Figure 5b, we choose typical model parameters for soft states. One can see that the jet contribution is negligible. There are many observations in the literature which show the correlation between observed spectral states with the jet (Fender et al. 2004; Belloni et al. 2005; Sriram et al. 2012). They also discussed correlations between the QPOs and the jet emissions in the HID diagram. All these correlations fall in place once the computation of the outflow rate to inflow rate ratio as a function of the properties of the centrifugal barrier was made (C99). The theoretical result directly shows that if indeed the outflows are produced from CENBOL, then, the soft and extremely hard states are going to produce very little outflows. Only intermediate states have higher outflow rates for a given inflow rate. When the optical depth is higher at the base of the jet, it produces blobby jets Chakrabarti et al. (2002); Nandi et al. (2001). In the soft state, due to cooling effects, this region is quenched and the mass outflow rate is reduced (see also, Garain et al. 2012). Recently, Jana et al. (2017) estimated the X-ray flux from the base of the jet for Swift J1753.5-0127 BHC using TCAF model.

Till now, we did not show the contribution of BMC component in the spectral plots. In Figure 6 we show the emitted spectrum when hard photons from the CENBOL pass through the outflowing diverging jet. In Figure 6, we show the spectral components including jet when the down-scattering effects of the CENBOL photons due to the bulk motion of the jet is considered. The black line shows the net spectrum when the BMC effect is also included, the blue and indigo lines show the jet component with BMC effect respectively. Here, green and red lines are disk blackbody and thermal Comptonization spectra obtained from the original C97 solution. The net spectrum clearly shows a bump, which is slightly higher in JeTCAF spectra as compared to the TCAF. In, TS05 explained that the bump is due to the BMC effects of the CENBOL photons by the diverging outflows discussed in CT95. In the next Section, we use both TCAF and JeTCAF model to fit the observed data, where we find the signatures of the BMC effect.

4. GS 1354-64

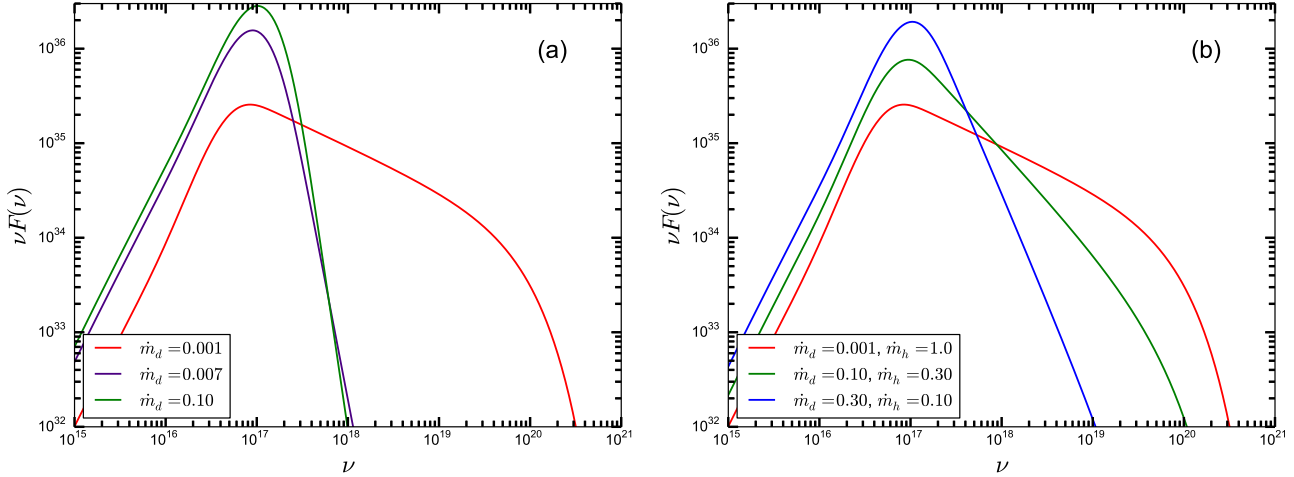


Figure 2. (a) Scattering of soft photons from the disk by the jet when disk accretion rate varies from 0.001 to 0.1 when halo rate is 1.0, keeping all other flow parameters fixed. The spectrum softens with increasing accretion rate. (b) Similar spectral variation as in (a) for different sets of disk and halo accretion rates, when other parameters are the same as in (a). The spectrum softens when the accretion rate changes to change the spectral state from hard to intermediate. Other parameters are $M_{\text{BH}}=10.0$, $X_s=20.0$, $R=2.5$ and $f_{\text{col}}=0.1$. Here, frequency is in Hz unit.

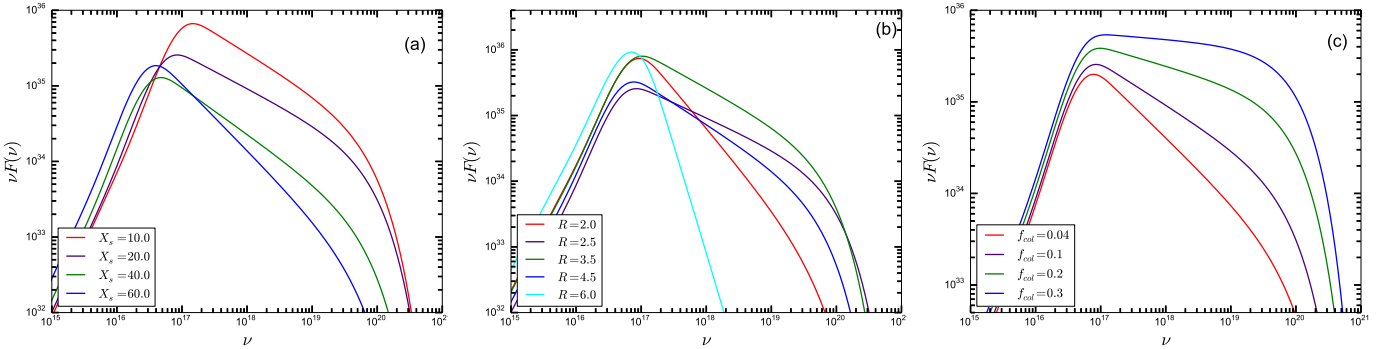


Figure 3. Same as Figure 2, (a) for varying size of the Compton cloud (X_s) when $R=2.5$ and $f_{\text{col}}=0.1$, (b) for different values of compression ratio R when $X_s=20.0$ and $f_{\text{col}}=0.1$, and (c) for different values of collimation factor (f_{col}) when $X_s=20.0$ and $R=2.5$. In (a), as the location/size increases, the spectrum becomes softer. In (b) as the value of R increases, mass outflow rate also increases, which increases the optical depth and the average number of the scattering. Thus, the spectrum becomes harder. However, mass outflow rate starts to decrease when R becomes higher than 4.5 and the spectrum again gets softer. This can be seen for $R = 6.0$. In (c), spectrum becomes harder with increasing collimation factor. The other parameters for both the plots are $M_{\text{BH}}=10.0$, $\dot{m}_d=0.001$, and $\dot{m}_h=1.0$.

We now use our computed spectra to fit the data of the black hole candidate GS 1354-64. GS 1354-64 is a dynamically confirmed low mass X-ray binary with a black hole mass $> 7 M_{\odot}$, ~ 2.5 day orbital period, and a distance of $\sim 25 - 61$ kpc (Casares et al. 2004, 2009). Reynolds & Miller (2011) reported the possible distance to be ~ 15 kpc and this large difference is due to the extinction effects. Very recently, Gandhi et al. (2019) estimated the distance of this source to be less than or around 1 kpc from Gaia DR2 observation. The DR2 distance would make the source under-luminous in both optical and X-ray wavebands. Apart from that, a

large discrepancy also makes a large uncertainty in estimating the donor star classification and its intrinsic brightness. This candidate showed two confirmed outbursts: one in 1987 (Makino 1987), when the source entered into the soft state (Kitamoto et al. 1990) and in 1997 (Brockopp et al. 2001), when the source was in a pure hard state (Revnivtsev et al. 2000). In the same outburst for the first time, Fender et al. (1997) observed a radio counterpart. In late May 2015, the optical brightness of this source was twice higher than the quiescent values reported by Russell & Lewis (2015). Recently, Koljonen et al. (2016) showed that the source

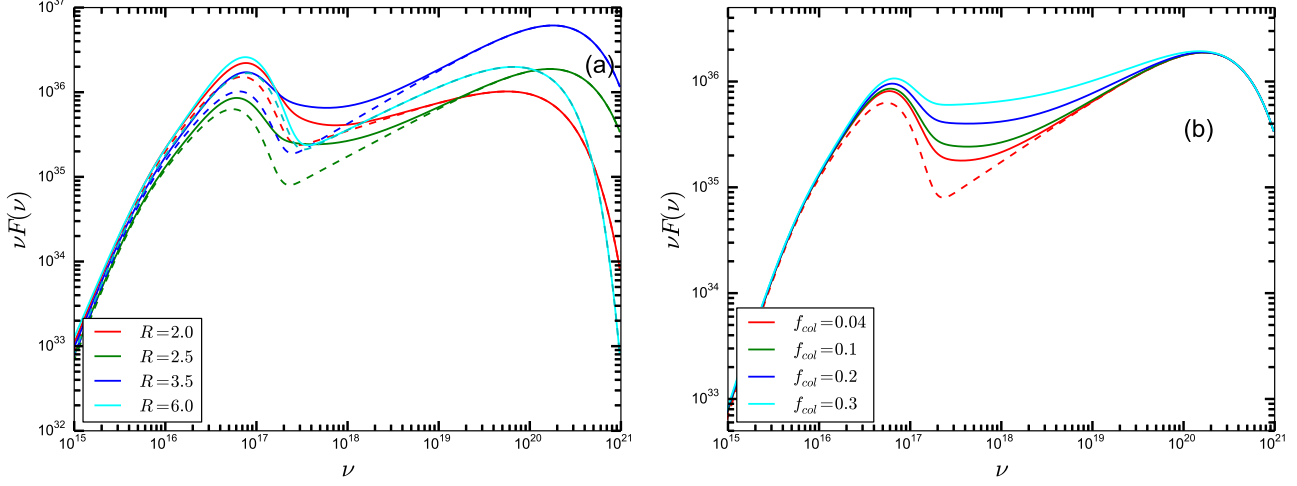


Figure 4. (a) Total emitted spectra with (solid lines) and without the jet contribution (dashed lines, same as TCAF spectra), for different values of R , and (b) f_{col} . In (a), we see that the spectrum becomes harder with increasing R . The new parameter (f_{col}) does not affect the CENBOL spectrum and thus the total spectrum without the jet contribution is the same for all (dashed line). The other parameters are $M_{\text{BH}}=10.0 M_{\odot}$, $\dot{m}_d = 0.001$, $\dot{m}_h = 1.0$ and $X_s = 20.0$. Here, frequency is in Hz unit.

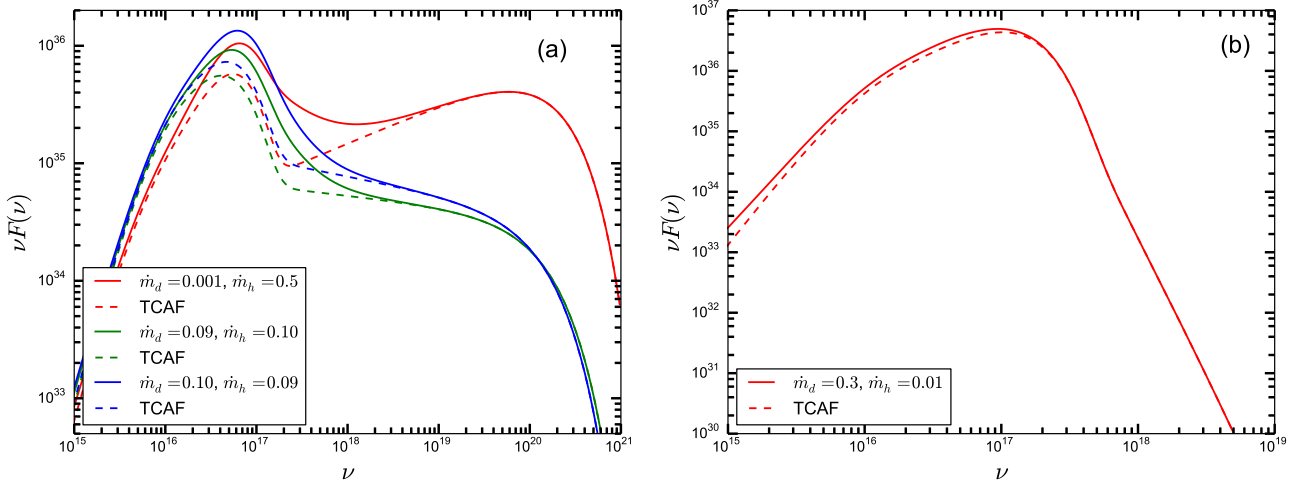


Figure 5. (a) Total emitted spectrum with (solid lines) and without (dashed lines) jet contribution for different spectral states depending on the accretion rates when other parameters are fixed ($X_s = 20.0$ and $R = 3.0$). There is a significant change in the spectrum as compared with the soft state in presence of jet. (b) Total spectrum in the soft state in presence of jet (solid line) component when $X_s = 10.0$ and $R = 1.2$. In the soft state, the jet contribution is negligible and both the spectra are the same. For both the plots $M_{\text{BH}}=10.0$ and $f_{\text{col}} = 0.2$. Here, frequency is in Hz unit.

has again entered into the hard state, studying multi-wavelength observation during its 2015 outburst. They also confirmed that optical/UV are tightly correlated with X-ray, which is consistent with the emission from the jet.

We consider the *NuSTAR* (Harrison et al. 2013) observation of 2015 June 13 (90101006002, hereafter X02) and July 11 (X04) outbursts. We consider FPMA observation with 4.0-65.0 keV energy range data. The exposure times for these observations are ~ 24 ks and

~ 30 ks respectively. For pipeline reduction and spectral file generation we use *nupipeline* and *nuproducts* tasks. After successfully processing the data we do spectral fitting using (1) *Tbabs** (*Gauss*+*TCAF*), and (2) *Tabs** (*Gauss*+*JeTCAF*). We follow the standard data extraction procedures using *NuSTARDAS* and *HEASoft* packages and the spectral fitting using *XSPEC*. The detail of the analysis procedure and the related fitting issues are discussed in Mondal & Chakrabarti (2019). For the spectral fitting of X02, we use TCAF model gener-

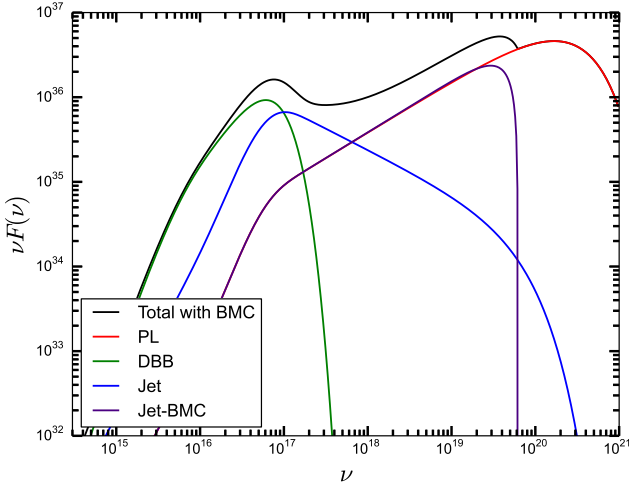


Figure 6. Different components including the jet which contribute to the net spectrum. Black line shows the total spectrum with a jet, the blue line is the jet component and the indigo line indicates the BMC effect of the outgoing jet. Red and green lines show thermal Comptonization and black-body spectra as in the original TCAF solution. The disk and the jet parameters for this plot are $M_{\text{BH}}=10.0$, $\dot{m}_d = 0.001$, $\dot{m}_h = 1.0$, $X_s = 20.0$, $R = 3.0$ and $f_{\text{col}} = 0.1$. Here, frequency is in Hz unit.

ated *fits* file (Debnath et al. 2014) as a local additive table model, following *atable* command in XSPEC. For the generation of model fit file, large no of spectra are generated for the range between $10^{14} - 10^{21}$ Hz. During the fitting, we keep the black hole mass as a free parameter and for both the observations we keep N_H fixed at $0.5 \times 10^{22} \text{ cm}^{-2}$ following HEASARC column density tool (Dickey & Lockman 1990). Data fitting with TCAF gives a very good fit with reduced $\chi^2 = 1.046$. After successful fitting, we get the value of $M_{\text{BH}} = 7.22^{+0.25}_{-0.89}$. In Figure 7, we show the TCAF model fitted spectra of X02.

For the fitting of X04, first, we attempt to fit the data using TCAF model generated *fits* file. We tried with different combinations of model parameters, however, the quality of the fit is poor, with a reduced χ^2 value > 2.5 , as that version of the *fits* file does not include the jet contribution. After this, we fit the data with JeTCAF model keeping all parameters free provided the N_H . We see that JeTCAF model fits the observed data with a much better statistics. In this case, we run the *source code* directly in XSPEC as a table model using *initpackage* and *lmod* tools (Arnaud 1996). The model parameters range used in *lmod* to run JeTCAF in XSPEC is shown in Table 1. The range of energy considered for the generation of model spectrum to fit

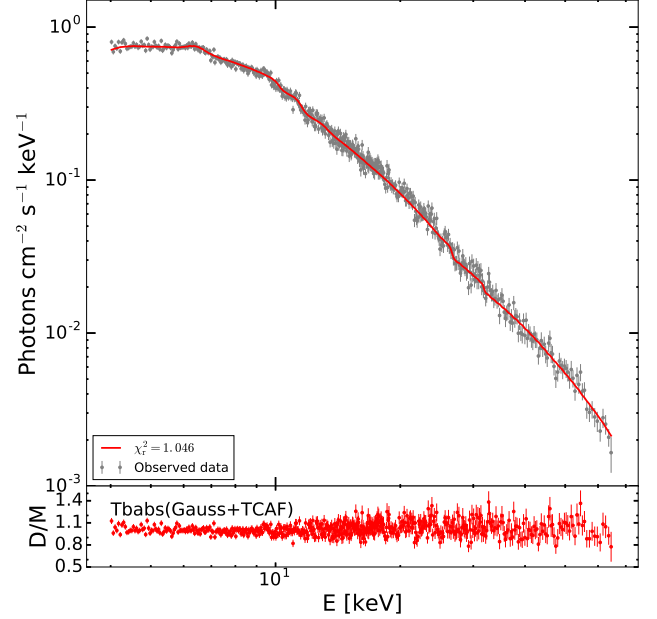


Figure 7. *NuSTAR* FPMA data (X02) of GS 1354-64, fitted with TCAF model as a local additive table model. Gray points with error bar shows the observed data and red line is the model spectrum. Data/model (D/M) ratio is shown in the lower panel. Data are rebinned for clarity.

the data is between $10^{17} - 10^{20}$ Hz. For both the models we assumed accretion efficiency 0.1.

In Figure 8, we show the JeTCAF model fitted spectra. In the upper panel, the red curve shows the JeTCAF model spectrum and the gray dots with error bars show the observed spectra. In the lower panel, we show the ratio of data and model, which shows a good agreement of fit with a reduced $\chi^2 = 1.112$. For comparison with TCAF model fit to the data, we overplotted the model spectrum (green line) and corresponding D/M ratio (in green) in the bottom panel. The model fitted parameters are shown in Table 2 for both X02 and X04 observations. The model fitted mass of the black hole for X04 is $6.7^{+0.54}_{-0.68}$. Comparing mass obtained from both the observations, we conclude that the mass of the central black hole is $\sim 7 M_{\odot}$. After reaching a good fit, we use the model fitted parameters to recalculate the energy spectral index (α) for X02 and X04. The calculated value of α for X02 and X04 are 0.63 and 0.87 respectively. The values of α and accretion rates confirm that on X02 day the source was in the “hard spectral state” and on X04 day it was in the “intermediate spectral state” when the jet was observed. The ratio of outflowing and inflowing matter rate for this observation is $0.12^{+0.02}_{-0.03}$, recalculated from the model fitted parameters using Eq. 1. The estimation of error in $R_{\dot{m}}$ measurement is discussed in Appendix. The above value of mass loss rate and the values

Table 2. Best fitted Gauss+TCAF and Gauss+JeTCAF model fitted parameters. The Gaussian model fitted line energy is E_g and width is σ_g . Here, N_g is the Gaussian model normalization in Photons $\text{cm}^{-2} \text{s}^{-1}$ unit.

Parameters	TCAF	JeTCAF
	X02	X04
E_g [keV]	$6.40^{+0.06}_{-0.06}$	$6.45^{+0.05}_{-0.06}$
σ_g [keV]	$0.24^{+0.06}_{-0.07}$	$0.60^{+0.04}_{-0.04}$
$N_g [10^{-4}]$	$1.41^{+0.22}_{-0.25}$	$17.28^{+1.17}_{-1.05}$
$M_{\text{BH}} [M_\odot]$	$7.22^{+0.25}_{-0.89}$	$6.70^{+0.54}_{-0.68}$
$\dot{m}_d [\dot{M}_{\text{Edd}}]$	$0.038^{+0.005}_{-0.003}$	$0.084^{+0.003}_{-0.003}$
$\dot{m}_h [\dot{M}_{\text{Edd}}]$	$1.346^{+0.092}_{-0.076}$	$0.265^{+0.009}_{-0.013}$
$X_s [r_g]$	$140.24^{+18.07}_{-5.89}$	$37.74^{+3.49}_{-2.74}$
R	$1.94^{+0.13}_{-0.18}$	$4.22^{+0.19}_{-0.28}$
f_{col}	—	$0.47^{+0.09}_{-0.09}$
	$\chi_r^2 = 1.046$	$\chi_r^2 = 1.112$

of R during the outburst, which is common in centrifugally driven flows (Molteni et al. 1994, C99), show the strong signature of an outflowing jet. Our model fitted mass is well within the range reported earlier for this source.

Earlier reports confirmed this outburst as a “failed outburst” due to the presence of only hard state (El-Batal et al. 2016; Stiele & Kong 2016). From our model fitted parameters, α value and high mass outflow rate, we identify the spectral state to be a hard (intermediate) state, like earlier findings. It is to be noticed that disk accretion rate increased by ~ 2.2 times, and entered into the region from where catastrophic cooling becomes significant according to TCAF. As we discussed earlier, from the model fitted parameters, mass loss rate, and energy spectral index, we confirm the presence of both hard and intermediate states.

This candidate showed a low-frequency QPO (~ 0.2 Hz) with increasing centroid frequency (Koljonen et al. 2016), which might be the indication of some instability occurring periodically. From the high flux behavior several authors argued this source to be similar to GRS 1915+105. Another possibility could be a periodic feedback from jet (Chakrabarti et al. 2002; Vadawale et al. 2001). There is no detailed dynamical lightcurve analysis on this topic till date. If we consider the burst time (t_{b-b}) theory of C99 and estimate the periodicity of the burst from the model fitted parameters, it gives ~ 20 sec (see Eq. 24 of C99). The t_{b-b} value can also be estimated from the observed QPO frequency for this source (0.2 Hz), using (C99) $t_{b-b} \propto \nu_{\text{QPO}}^{-2} \sim 25$ s. Both estimates are consistent with each other. This estimate also matches with 20 s peri-

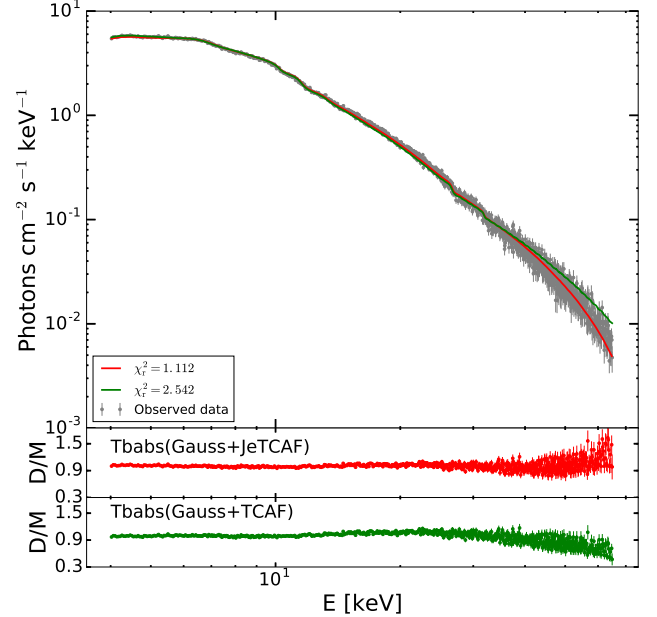


Figure 8. *NuSTAR* FPMA data (X04) of GS 1354-64, fitted with JeTCAF model as a local model directly in XSPEC. Gray points with error bars show the observed data and the red line is the model spectrum. The green line shows the TCAF model spectrum for comparison with JeTCAF model. The difference can be noted between $\sim 15 - 25$ keV and near the tail of the spectrum due to BMC of the photons scattered off the base of the jet. Data/model (D/M) ratio is shown in lower panels. Data are rebinned for clarity.

odicity observed in the lightcurve of this source during *RXTE* era (see Fig. 2 of Janiuk & Czerny 2011). There are several works in the literature (Belloni et al. 2000; Rao et al. 2000; Naik et al. 2002; Chakrabarti et al. 2004; Pal & Chakrabarti 2015) which discussed changes in different classes of lightcurves in black hole candidates in a matter of few seconds. Such quick transitions are possible only if the changes in accretion/ejection processes are due to local effects at the base of the jet or due to the return flow onto the disk (e.g., see Chakrabarti et al. 2002), whereas burst-on and burst-off states of GRS 1915+105 were discussed as due to interacting outflow with the inner disk. Here we suggested cycles inside a lightcurve due to the feedback effects from the outflows in a timescale of 20 sec. It is possible and is seen in GRS 1915+105 and IGR 17091-3624 (Belloni et al. 2000; Rothstein et al. 2005; Pal & Chakrabarti 2015) very often. There has to be changes in the local disk rather than the global disk.

5. SUMMARY AND CONCLUSIONS

In this paper, we study the spectral properties of the accretion flows around black holes when the jet is also included in the TCAF solution. We apply this JeT-

CAF solution to study the transient source GS 1354-64 during its 2015 outburst using the data from *NuSTAR* satellite. We treat the base of the jet to be an additional Compton cloud component which also scatters soft photons from the disk. We also include the effects of bulk motion of the diverging jet. Our jet configuration is self-consistent with the accretion dynamics in the sense that it estimates mass loss solving flow equations, rather than considering it separately. In this model, the jet is originated from the post-shock region (CENBOL) of the flow, and the velocity of the outflowing matter is calculated from the average temperature of the CENBOL. We estimate the mass outflow rate from the inflow rate. We use a realistic outflow to obtain the optical depth and the temperature of the Compton cloud. The mass outflow rate and the velocity are high in hard and intermediate states, thus the jet contribution to the spectrum is also modified significantly (due to bulk motion) during that time. In the soft state, the temperature is not high enough to accelerate the mass outflow. Thus, the spectrum remains nearly blackbody. We also see that the contribution of the jet to the overall spectrum varies with the size of the Compton cloud, the shock compression ratio and the jet collimation factor. The overall fits using our simple consideration is acceptable, and we do not require presence of magnetic field or synchrotron emission to fit the data.

In this manuscript, we applied the model on the BHC GS 1354-64 and calculated the mass outflow rate during its 2015 outburst. In future, we aim to consider other jetted candidates using the same model. Our study shows that during the outburst, this candidate had a ratio of mass outflow to mass inflow rate of about $0.12^{+0.02}_{-0.03}$. We suspect the reason behind the presence of very low QPO frequency with varying centroid frequency is also an indication of micro outbursts or feedback from jet to the disk occurring in very small-time scales (20 sec). This is similar to what happened in

GRS 1915+105 (also in IGR 17091-3624). It is true that the spin of the black hole is important for both the disk and jet study, however its effects cannot spread beyond a few gravitational radii, while the physics we discuss is of farther out regions. As we discussed earlier, the spin may or may not contribute in powering the jet. However, the present TCAF or JeTCAF model does not consider the spin effect. In future, we aim to implement that effect self-consistently in the model. A further study of this object is required to understand the jet feedback mechanism, class transition in lightcurve to understand the dynamics of the disk.

6. ACKNOWLEDGMENT

We thank the referee for making insightful comments and suggestions. SM is thankful to Keith A. Arnaud for helping in model inclusion during his visit to NASA/GSFC as a student of COSPAR Capacity-building Workshop Fellowship program jointly with ISRO, India. SM acknowledges Ramanujan Fellowship (# RJF/2020/000113) by SERB-DST, Govt. of India for this research. This research has made use of the *NuSTAR* Data Analysis Software (NuSTARDAS) jointly developed by the ASI Science Data Center (ASDC, Italy) and the California Institute of Technology (Caltech, USA).

APPENDIX

For the estimation of error in $R_{\dot{m}}$, we derived the relation:

$$\sigma_{R_{\dot{m}}} = \sqrt{\left(\frac{\partial R_{\dot{m}}}{\partial R}\right)^2 \sigma_R^2 + \left(\frac{\partial R_{\dot{m}}}{\partial f_{\text{col}}}\right)^2 \sigma_{f_{\text{col}}}^2},$$

where, σ_R and $\sigma_{f_{\text{col}}}$ are the error in measurement of shock compression ratio (R) and collimation factor (f_{col}) respectively. After doing a few steps of algebra we get the value of $\frac{\partial R_{\dot{m}}}{\partial R} = -0.05$ and $\frac{\partial R_{\dot{m}}}{\partial f_{\text{col}}} = 0.24$, which give the value of $\sigma_{R_{\dot{m}}} = \{+0.02, -0.03\}$.

REFERENCES

- Arnaud, K. A. 1996, *Astronomical Society of the Pacific Conference Series*, Vol. 101, *XSPEC: The First Ten Years*, ed. G. H. Jacoby & J. Barnes, 17
- Belloni, T., Homan, J., Casella, P., et al. 2005, *A&A*, 440, 207, doi: [10.1051/0004-6361:20042457](https://doi.org/10.1051/0004-6361:20042457)
- Belloni, T., Migliari, S., & Fender, R. P. 2000, *A&A*, 358, L29. <https://arxiv.org/abs/astro-ph/0005307>
- Blandford, R., Meier, D., & Readhead, A. 2019, *ARA&A*, 57, 467, doi: [10.1146/annurev-astro-081817-051948](https://doi.org/10.1146/annurev-astro-081817-051948)
- Blandford, R. D., & Payne, D. G. 1981, *MNRAS*, 194, 1033, doi: [10.1093/mnras/194.4.1033](https://doi.org/10.1093/mnras/194.4.1033)
- . 1982, *MNRAS*, 199, 883, doi: [10.1093/mnras/199.4.883](https://doi.org/10.1093/mnras/199.4.883)
- Brockspoll, C., Jonker, P. G., Fender, R. P., et al. 2001, *MNRAS*, 323, 517, doi: [10.1046/j.1365-8711.2001.04193.x](https://doi.org/10.1046/j.1365-8711.2001.04193.x)
- Bromberg, O., Nakar, E., Piran, T., & Sari, R. 2011, *ApJ*, 740, 100, doi: [10.1088/0004-637X/740/2/100](https://doi.org/10.1088/0004-637X/740/2/100)
- Casares, J., Zurita, C., Shahbaz, T., Charles, P. A., & Fender, R. P. 2004, *ApJL*, 613, L133, doi: [10.1086/425145](https://doi.org/10.1086/425145)

- Casares, J., Orosz, J. A., Zurita, C., et al. 2009, *ApJS*, 181, 238, doi: [10.1088/0067-0049/181/1/238](https://doi.org/10.1088/0067-0049/181/1/238)
- Chakrabarti, S., & Titarchuk, L. G. 1995, *ApJ*, 455, 623, doi: [10.1086/176610](https://doi.org/10.1086/176610)
- Chakrabarti, S. K. 1989, *ApJ*, 347, 365, doi: [10.1086/168125](https://doi.org/10.1086/168125)
- . 1996, *ApJ*, 464, 664, doi: [10.1086/177354](https://doi.org/10.1086/177354)
- . 1997, *ApJ*, 484, 313, doi: [10.1086/304325](https://doi.org/10.1086/304325)
- . 1999, *A&A*, 351, 185.
<https://arxiv.org/abs/astro-ph/9910014>
- Chakrabarti, S. K., Nandi, A., Choudhury, A., & Chatterjee, U. 2004, *ApJ*, 607, 406, doi: [10.1086/383235](https://doi.org/10.1086/383235)
- Chakrabarti, S. K., Nandi, A., Manickam, S. G., Mandal, S., & Rao, A. R. 2002, *ApJL*, 579, L21, doi: [10.1086/344783](https://doi.org/10.1086/344783)
- Chatterjee, D., Debnath, D., Chakrabarti, S. K., Mondal, S., & Jana, A. 2016, *ApJ*, 827, 88, doi: [10.3847/0004-637X/827/1/88](https://doi.org/10.3847/0004-637X/827/1/88)
- Chattopadhyay, I., Das, S., & Chakrabarti, S. K. 2004, *MNRAS*, 348, 846, doi: [10.1111/j.1365-2966.2004.07398.x](https://doi.org/10.1111/j.1365-2966.2004.07398.x)
- Debnath, D., Chakrabarti, S. K., & Mondal, S. 2014, *MNRAS*, 440, L121, doi: [10.1093/mnrasl/slu024](https://doi.org/10.1093/mnrasl/slu024)
- Debnath, D., Mondal, S., & Chakrabarti, S. K. 2015, *MNRAS*, 447, 1984, doi: [10.1093/mnras/stu2588](https://doi.org/10.1093/mnras/stu2588)
- Dickey, J. M., & Lockman, F. J. 1990, *ARA&A*, 28, 215, doi: [10.1146/annurev.aa.28.090190.001243](https://doi.org/10.1146/annurev.aa.28.090190.001243)
- Done, C., Davis, S. W., Jin, C., Blaes, O., & Ward, M. 2012, *MNRAS*, 420, 1848, doi: [10.1111/j.1365-2966.2011.19779.x](https://doi.org/10.1111/j.1365-2966.2011.19779.x)
- Done, C., Gierliński, M., & Kubota, A. 2007, *A&A Rv*, 15, 1, doi: [10.1007/s00159-007-0006-1](https://doi.org/10.1007/s00159-007-0006-1)
- D'Silva, S., & Chakrabarti, S. K. 1994, *ApJ*, 424, 149, doi: [10.1086/173879](https://doi.org/10.1086/173879)
- Ebisawa, K., Życki, P., Kubota, A., Mizuno, T., & Watarai, K.-y. 2003, *ApJ*, 597, 780, doi: [10.1086/378586](https://doi.org/10.1086/378586)
- Eggum, G. E., Coroniti, F. V., & Katz, J. I. 1988, *ApJ*, 330, 142, doi: [10.1086/166462](https://doi.org/10.1086/166462)
- El-Batal, A. M., Miller, J. M., Reynolds, M. T., et al. 2016, *ApJL*, 826, L12, doi: [10.3847/2041-8205/826/1/L12](https://doi.org/10.3847/2041-8205/826/1/L12)
- Fender, R. P., Belloni, T. M., & Gallo, E. 2004, *MNRAS*, 355, 1105, doi: [10.1111/j.1365-2966.2004.08384.x](https://doi.org/10.1111/j.1365-2966.2004.08384.x)
- Fender, R. P., Gallo, E., & Russell, D. 2010, *MNRAS*, 406, 1425, doi: [10.1111/j.1365-2966.2010.16754.x](https://doi.org/10.1111/j.1365-2966.2010.16754.x)
- Fender, R. P., Homan, J., & Belloni, T. M. 2009, *MNRAS*, 396, 1370, doi: [10.1111/j.1365-2966.2009.14841.x](https://doi.org/10.1111/j.1365-2966.2009.14841.x)
- Fender, R. P., Tingay, S. J., Higdon, J., Wark, R., & Wieringa, M. 1997, *IAUC*, 6779, 2
- Gandhi, P., Rao, A., Johnson, M. A. C., Paice, J. A., & Maccarone, T. J. 2019, *MNRAS*, 485, 2642, doi: [10.1093/mnras/stz438](https://doi.org/10.1093/mnras/stz438)
- Garain, S. K., Balsara, D. S., Chakrabarti, S. K., & Kim, J. 2020, *ApJ*, 888, 59, doi: [10.3847/1538-4357/ab5d3c](https://doi.org/10.3847/1538-4357/ab5d3c)
- Garain, S. K., Ghosh, H., & Chakrabarti, S. K. 2012, *ApJ*, 758, 114, doi: [10.1088/0004-637X/758/2/114](https://doi.org/10.1088/0004-637X/758/2/114)
- Harrison, F. A., Craig, W. W., Christensen, F. E., et al. 2013, *ApJ*, 770, 103, doi: [10.1088/0004-637X/770/2/103](https://doi.org/10.1088/0004-637X/770/2/103)
- Hjellming, R. M., & Rupen, M. P. 1995, *Nature*, 375, 464, doi: [10.1038/375464a0](https://doi.org/10.1038/375464a0)
- Jana, A., Chakrabarti, S. K., & Debnath, D. 2017, *ApJ*, 850, 91, doi: [10.3847/1538-4357/aa88a5](https://doi.org/10.3847/1538-4357/aa88a5)
- Janiuk, A., & Czerny, B. 2011, *MNRAS*, 414, 2186, doi: [10.1111/j.1365-2966.2011.18544.x](https://doi.org/10.1111/j.1365-2966.2011.18544.x)
- Kawashima, T., Ohsuga, K., Mineshige, S., et al. 2012, *ApJ*, 752, 18, doi: [10.1088/0004-637X/752/1/18](https://doi.org/10.1088/0004-637X/752/1/18)
- King, A. R., Davies, M. B., Ward, M. J., Fabbiano, G., & Elvis, M. 2001, *ApJL*, 552, L109, doi: [10.1086/320343](https://doi.org/10.1086/320343)
- Kitamoto, S., Tsunemi, H., Pedersen, H., Ilovaisky, S. A., & van der Klis, M. 1990, *ApJ*, 361, 590, doi: [10.1086/169222](https://doi.org/10.1086/169222)
- Koljonen, K. I. I., Russell, D. M., Corral-Santana, J. M., et al. 2016, *MNRAS*, 460, 942, doi: [10.1093/mnras/stw1007](https://doi.org/10.1093/mnras/stw1007)
- Makino, F. 1987, *IAUC*, 4342, 1
- Miller-Jones, J. C. A., Sivakoff, G. R., Altamirano, D., et al. 2012, *MNRAS*, 421, 468, doi: [10.1111/j.1365-2966.2011.20326.x](https://doi.org/10.1111/j.1365-2966.2011.20326.x)
- Mirabel, I. F., & Rodríguez, L. F. 1998, *Nature*, 392, 673, doi: [10.1038/33603](https://doi.org/10.1038/33603)
- Molteni, D., Lanzafame, G., & Chakrabarti, S. K. 1994, *ApJ*, 425, 161, doi: [10.1086/173972](https://doi.org/10.1086/173972)
- Mondal, S., & Chakrabarti, S. K. 2013, *MNRAS*, 431, 2716, doi: [10.1093/mnras/stt361](https://doi.org/10.1093/mnras/stt361)
- . 2019, *MNRAS*, 483, 1178, doi: [10.1093/mnras/sty3169](https://doi.org/10.1093/mnras/sty3169)
- Mondal, S., Chakrabarti, S. K., & Debnath, D. 2014a, *Ap&SS*, 353, 223, doi: [10.1007/s10509-014-2008-6](https://doi.org/10.1007/s10509-014-2008-6)
- Mondal, S., Chakrabarti, S. K., Nagarkoti, S., & Arévalo, P. 2017, *ApJ*, 850, 47, doi: [10.3847/1538-4357/aa7e27](https://doi.org/10.3847/1538-4357/aa7e27)
- Mondal, S., Debnath, D., & Chakrabarti, S. K. 2014b, *ApJ*, 786, 4, doi: [10.1088/0004-637X/786/1/4](https://doi.org/10.1088/0004-637X/786/1/4)
- Nagarkoti, S., & Chakrabarti, S. K. 2016, *MNRAS*, 462, 850, doi: [10.1093/mnras/stw1700](https://doi.org/10.1093/mnras/stw1700)
- Naik, S., Rao, A. R., & Chakrabarti, S. K. 2002, *Journal of Astrophysics and Astronomy*, 23, 213, doi: [10.1007/BF02702284](https://doi.org/10.1007/BF02702284)
- Nandi, A., Chakrabarti, S. K., Vadawale, S. V., & Rao, A. R. 2001, *A&A*, 380, 245, doi: [10.1051/0004-6361:20011444](https://doi.org/10.1051/0004-6361:20011444)
- Narayan, R., & McClintock, J. E. 2012, *MNRAS*, 419, L69, doi: [10.1111/j.1745-3933.2011.01181.x](https://doi.org/10.1111/j.1745-3933.2011.01181.x)
- Nobili, L., Turolla, R., & Zampieri, L. 1993, *ApJ*, 404, 686, doi: [10.1086/172322](https://doi.org/10.1086/172322)

- Ohsuga, K., Mori, M., Nakamoto, T., & Mineshige, S. 2005, *ApJ*, 628, 368, doi: [10.1086/430728](https://doi.org/10.1086/430728)
- Okuda, T. 2002, *PASJ*, 54, 253, doi: [10.1093/pasj/54.2.253](https://doi.org/10.1093/pasj/54.2.253)
- Pahari, M., Gandhi, P., Charles, P. A., et al. 2017, *MNRAS*, 469, 193, doi: [10.1093/mnras/stx840](https://doi.org/10.1093/mnras/stx840)
- Pal, P. S., & Chakrabarti, S. K. 2015, *Advances in Space Research*, 56, 1784, doi: [10.1016/j.asr.2015.07.016](https://doi.org/10.1016/j.asr.2015.07.016)
- Radhika, D., & Nandi, A. 2014, *Advances in Space Research*, 54, 1678, doi: [10.1016/j.asr.2014.06.039](https://doi.org/10.1016/j.asr.2014.06.039)
- Rao, A. R., Yadav, J. S., & Paul, B. 2000, *ApJ*, 544, 443, doi: [10.1086/317168](https://doi.org/10.1086/317168)
- Revnivtsev, M. G., Borozdin, K. N., Friedhorsky, W. C., & Vikhlinin, A. 2000, *ApJ*, 530, 955, doi: [10.1086/308386](https://doi.org/10.1086/308386)
- Reynolds, M. T., & Miller, J. M. 2011, *ApJL*, 734, L17, doi: [10.1088/2041-8205/734/1/L17](https://doi.org/10.1088/2041-8205/734/1/L17)
- Rothstein, D. M., Eikenberry, S. S., & Matthews, K. 2005, *ApJ*, 626, 991, doi: [10.1086/429217](https://doi.org/10.1086/429217)
- Russell, D. M., & Lewis, F. 2015, *The Astronomer's Telegram*, 7637, 1
- Shakura, N. I., & Sunyaev, R. A. 1973, *A&A*, 500, 33
- Singh, C. B., & Chakrabarti, S. K. 2011, *MNRAS*, 410, 2414, doi: [10.1111/j.1365-2966.2010.17615.x](https://doi.org/10.1111/j.1365-2966.2010.17615.x)
- Sriram, K., Rao, A. R., & Choi, C. S. 2012, *A&A*, 541, A6, doi: [10.1051/0004-6361/201218799](https://doi.org/10.1051/0004-6361/201218799)
- Stiele, H., & Kong, A. K. H. 2016, *MNRAS*, 459, 4038, doi: [10.1093/mnras/stw903](https://doi.org/10.1093/mnras/stw903)
- Sunyaev, R. A., & Titarchuk, L. G. 1980, *A&A*, 500, 167
- Titarchuk, L., Kazanas, D., & Becker, P. A. 2003, *ApJ*, 598, 411, doi: [10.1086/378701](https://doi.org/10.1086/378701)
- Titarchuk, L., & Shrader, C. 2005, *ApJ*, 623, 362, doi: [10.1086/424918](https://doi.org/10.1086/424918)
- Titarchuk, L., & Zannias, T. 1998, *ApJ*, 493, 863, doi: [10.1086/305157](https://doi.org/10.1086/305157)
- Vadawale, S. V., Rao, A. R., Nandi, A., & Chakrabarti, S. K. 2001, *A&A*, 370, L17, doi: [10.1051/0004-6361:20010318](https://doi.org/10.1051/0004-6361:20010318)